JOURNAL OF SOLID STATE CHEMISTRY **124,** 143–150 (1996)
ARTICLE NO. 0217

Polarized Electronic Absorption Spectra of Tetrahedrally Coordinated Co^{2+} Ions in the New Compound $Ca_3Co(SeO_3)_4$ and Its Structural Characterization

M. Wildner[1]

Institut für Mineralogie und Kristallographie, Technische Universität Berlin, Ernst-Reuter-Platz 1, D-10587 Berlin, Germany

Received November 13, 1995; accepted March 11, 1996

The crystal structure of the new compound $Ca_3Co(SeO_3)_4$ was investigated using single crystal X-ray diffraction data up to $\sin\theta/\lambda = 0.86$ [tetragonal, space group $I4_1/a$, $a = 7.571(1)$, $c = 22.493(3)$ Å, $Z = 4$; $R1 = 0.024$ for $1125 F_0 > 4\sigma(F_0)$ and 47 variables]. The structure is composed of nearly perfectly regular CoO_4 tetrahedra, pyramidal SeO_3 groups, and two types of CaO_8 polyhedra. $Ca_3Co(SeO_3)_4$ represents the first example for a selenite compound containing CoO_4 tetrahedra. Furthermore, polarized electronic absorption spectra of $Ca_3Co(SeO_3)_4$ in the range from 2000 to 35,000 cm^{-1} were obtained by means of UV/VIS microscope- and FTIR-spectrometry. The observed strong polarization of the spectra is in contradiction to the regular shape of the CoO_4 tetrahedron and indicates a significant tetragonal field perturbation imposed by the further coordination of the CoO_4 group. The band positions, band widths, and splittings are interpreted based on crystal field calculations employing the crystal field parameters *Dq*, *Dt*, *Ds*, the Racah parameters *B* and *C*, and the spin–orbit coupling constant ζ. A rather good agreement of observed and calculated energies is obtained for a parameter set with $Dq = 395$, $Dt = 25$, $Ds = 250$, $B = 770$, $C = 3400$, and $\zeta = 500$ cm^{-1}.

INTRODUCTION

The crystal chemistry of Co^{2+} selenites is characterized by the stereochemical individuality of the pyramidal SeO_3 groups and, up to now, by more or less distorted octahedral environments around Co^{2+} ions [cf. (1, 2) and references therein, and (3)]. As a part of this paper, the structural characterization of the novel compound $Ca_3Co(SeO_3)_4$ provides the first example for a selenite containing Co^{2+} ions in tetrahedral coordination. Furthermore, in view of the high symmetry [Co point symmetry $\bar{4}(S_4)$] and the practically ideal tetrahedral shape of the CoO_4 polyhedra, it seemed very promising to investigate the electronic absorption spectra of this new compound for several reasons. While a vast number of papers report electronic absorption spectra of (pseudo-)tetrahedral Co^{2+} ions [comprehensive listings can be found in (4) and (5)], only some provide polarized single crystal data, and only a few of them deal with oxygen coordination around cobalt. In most cases, the first spin-allowed transition which is predicted in the mid-IR region and which directly determines the value of the crystal field strength *Dq* has not been searched for or is masked by intense vibrational absorptions of polyatomic ligands. This is not expected in the case of $Ca_3Co(SeO_3)_4$, thus allowing the observation of this crystal field band. Metal–metal interactions are also precluded in the title compound judging from Co–Co distances of 6.78 Å. The present investigation also provides further crystal field data for transition metal ions incorporated in crystal structures of selenite compounds (1, 6, 7) and gives a comparison with corresponding data of oxides and other oxygen based structures of Co^{2+}.

EXPERIMENTAL

Single crystals of $Ca_3Co(SeO_3)_4$ up to ~0.8 mm were prepared under low-hydrothermal conditions. An appropriate mixture of SeO_2, $Co(OH)_2$, and $Ca(OH)_2$ was inserted together with some drops of water in Teflon coated steel vessels (capacity 4 cm^3, filling degree ~20%). This starting mixture had pH ~5. The closed vessels were kept at 220°C for 6 days and then cooled to room temperature within 24 h. In addition to single crystals of $Ca_3Co(SeO_3)_4$, an unidentified microcrystalline phase (~1 vol%) as well as few single crystals ($\ll$0.1 vol%) of a further new Ca–Co selenite, $Ca_2Co(SeO_3)_2(SeO_2OH)_2$, were obtained. Crystals of $Ca_3Co(SeO_3)_4$ have tetragonal dipyramidal habit; in incident light their color is a dark bluish violet, and in transmitted polarized light intense blue (E vector $\perp c$) to dull turquoise colors (E vector $\| c$) are observed.

Single crystal X-ray diffraction intensities were mea-

[1] Permanent and correspondence address: Institut für Mineralogie und Kristallographie, Universität Wien, Althanstraße 14, A-1090 Wien, Austria.

0022-4596/96 $18.00

TABLE 1
Summary of Crystal Data and Details of the X-ray Measurement and Structure Refinement of $Ca_3Co(SeO_3)_4$

Chemical formula	$Ca_3Co(SeO_3)_4$
M_r	687.0
Space group	$I4_1/a$ (No. 88, C_{4h}^6)
a [Å]	7.571(1)
c [Å]	22.493(3)
V [Å^3]	1289.3
Z	4
ρ_{calc} [g cm^{-3}]	3.539
μ(Mo$K\alpha$) [cm^{-1}]	138.7
Crystal dimensions [mm]	$0.3 \times 0.1 \times 0.1$
Extinction coefficient	1.09×10^{-3}
$2\theta_{max}$ [°]	75
Measured reflections	3863
Unique data set	1708
Variables	47
Transmission factors (ψ-scans)	0.26–0.34
$R1$ [for $1125 F_0 > 4\sigma(F_0)$]	0.024
$wR2$ [for all F_0^2]	0.046
Goodness of fit	0.928

Note. $R1 = \Sigma \|\|F_0| - |F_c\|| / \Sigma |F_0|$, $wR2 = [\Sigma w(F_0^2 - F_c^2)^2 / \Sigma w F_0^4]^{1/2}$, $w = 1/[\sigma^2(F_0^2) + (0.0104 \times P)^2]$, $P = \{[\max \text{ of } (0 \text{ or } F_0^2)] + 2F_c^2\}/3$.

sured at room temperature on a Stoe AED2 four-circle diffractometer with graphite monochromatized Mo$K\alpha$ radiation. Lattice constants were refined from 32 accurate 2θ values in the range $39° < 2\theta < 42°$. The space group was unequivocally fixed by systematic extinctions as $I4_1/a$ (No. 88, C_{4h}^6). The intensity data were corrected for Lorentz and polarization effects as well as for absorption using ψ-scan data. The structure was solved by direct methods (8); oxygen positions were obtained by subsequent Fourier syntheses. Crystal data and further information concerning the data collection and structure refinement are given in Table 1. Table 2 lists refined atomic coordinates and equivalent displacement parameters. For the refinement on F_0^2 and all further calculations SHELXL-93 (9) was used. Tables of observed and calculated structure factors and anisotropic displacement parameters are available from the author.

TABLE 2
Atomic Coordinates and Equivalent Displacement Parameters [pm^2] in $Ca_3Co(SeO_3)_4$

	x	y	z	U_{eq}
Ca(1)	0	$\frac{1}{4}$	0.44878(2)	138
Ca(2)	0	$\frac{1}{4}$	$\frac{5}{8}$	140
Co	0	$\frac{1}{4}$	$\frac{1}{8}$	153
Se	0.32054(2)	0.41824(3)	0.19219(1)	136
O(1)	0.3536(2)	0.6207(2)	0.2200(1)	216
O(2)	0.1011(2)	0.4373(2)	0.1754(1)	198
O(3)	0.4184(2)	0.4451(2)	0.1262(1)	222

Single crystals suitable for spectroscopic investigations were smaller than ~0.3 mm; therefore microscope-spectrometric techniques (cf. 10) had to be applied using a Zeiss UMSP80 spectrometer in the range 35,000–5000 cm^{-1}. The preparation of a polished crystal slab containing the fourfold axis and the determination of the sample thickness were done in analogy to previous papers (e.g., 1, 6, 7). π- and σ-polarized absorption spectra were recorded with the electric light vector parallel and perpendicular, respectively, to the fourfold axis. Spectral band and step widths were both 1 nm in the UV and VIS and 16/10 nm in the NIR region; the measuring spot was 40 μm in diameter. In order to achieve a better signal/noise ratio, spectral regions with weak absorption in $Ca_3Co(SeO_3)_4$ (34,000–19,000 cm^{-1}) were first measured at a sample thickness of 273 μm, and then the sample was ground to 15 μm and remeasured (35,000–5000 cm^{-1}).

π- and σ-polarized FTIR absorption spectra in the range 5000–2000 cm^{-1} were obtained on a Perkin–Elmer 1760X spectrometer equipped with a gold wire grid polarizer. A suitable single crystal was ground from both sides to a thickness of ~240 μm (in this case estimated by comparison with a micrometer scale). For the measurements a beam condensor with CsI lenses and circular mounts with a measuring spot of 100 μm in diameter had to be used. The spectral resolution was 4 cm^{-1}.

Crystal field calculations including the parameters Dq, Racah B and C, the tetragonal parameters Dt and Ds, and spin–orbit coupling were performed using the Crystal Field Computer Package by Yeung and Rudowicz (11); some additional calculations were done with an own program (Wildner, unpublished).

RESULTS AND DISCUSSION

Crystal Structure

Bond lengths and selected bond angles in $Ca_3Co(SeO_3)_4$ are listed in Table 3. Figure 1 shows the crystal structure in a projection on (010). This new structure type is composed of pyramidal SeO_3 groups, nearly perfectly regular CoO_4 tetrahedra, and two crystallographically different kinds of CaO_8 polyhedra.

The selenium atoms, located on a general site, are typically one-sided pyramidal coordinated to three oxygen atoms, a consequence of the stereochemical activity of lone-pair electrons of the Se^{4+} atoms. The mean O–Se–O angle, 100.2°, is identical with an average value given in the literature (12), whereas the mean Se–O bond length is significantly shorter than the corresponding value cited in (12), 1.709 Å. The two short individual Se–O bonds are those to O(1) and O(3), which are shared with calcium

TABLE 3
Bond Lengths [Å] and Selected Bond Angles [°] in $Ca_3Co(SeO_3)_4$

Ca(1)–O(1)	2×	2.350(1)	Ca(2)–O(1)	4×	2.599(2)
–O(1)	2×	2.890(2)	–O(3)	4×	2.390(1)
–O(2)	2×	2.543(2)	⟨Ca(2)–O⟩		2.495
–O(3)	2×	2.325(2)			
⟨Ca(1)–O⟩		2.527			
Co–O(2)	4×	1.970(2)	O(2)–Co–O(2)′	2×	109.73(9)
			O(2)–Co–O(2)″	4×	109.34(5)
			⟨O–Co–O⟩		109.47
Se–O(1)	1×	1.675(1)	O(1)–Se–O(2)	1×	98.66(8)
–O(2)	1×	1.710(1)	O(1)–Se–O(3)	1×	98.88(8)
–O(3)	1×	1.672(2)	O(2)–Se–O(3)	1×	102.94(8)
⟨Se–O⟩		1.686	⟨O–Se–O⟩		100.16

atoms only. O(2)—with a longer bond to Se—forms the common corner with a CoO_4 tetrahedron and is also shared with Ca(1).

Tetrahedral coordination of oxygen atoms around Co^{2+} ions is not very frequently observed in purely inorganic crystal structures (cf. 13). $Ca_3Co(SeO_3)_4$ represents the first example for a selenite compound containing CoO_4 groups. According to the $\bar{4}$ site symmetry of the Co atom, the CoO_4 tetrahedra are aligned parallel to the *c* axis and may only be distorted by an elongation or compression along this axis. However, the CoO_4 tetrahedron is practically perfectly regular (Table 3) and the Co–O distance is in agreement with crystal chemical expectations (13).

Corner sharing between CoO_4 and SeO_3 polyhedra results in isolated $[Co(SeO_3)_4]$ groups, which are interconnected by the Ca(2) atoms (site symmetry $\bar{4}$) to sheets parallel (001). Further linkage within these sheets and the connection with neighboring sheets is formed by the Ca(1) atoms (site symmetry 2). Both calcium atoms are eightfold coordinated and their mean Ca–O bond lengths comply well with data from literature, e.g., 2.50 Å in (14).

The oxygen atoms in $Ca_3Co(SeO_3)_4$ are bound to four or three cations. O(1) has a strongly distorted tetrahedral environment formed by one Se, two Ca(1), and a Ca(2) atom; O(2) and O(3) have nearly planar [3]-coordinations, O(2) to Se, Co and Ca(1), O(3) to Se, Ca(1) and Ca(2). Bond valence calculations according to (15) yield 2.06, 2.00, and 2.15 valence units, respectively, for the three oxygen atoms. Bond valence sums calculated for the cations are 4.21 vu for Se, 1.89 vu for Co, and 2.06 and 2.00 vu, respectively, for the Ca atoms.

Electronic Absorption Spectra

Figure 2 shows the polarized electronic absorption spectra of $Ca_3Co(SeO_3)_4$ obtained by microscope-spectrometric techniques in the region from 35,000 to 5000 cm^{-1}; Figure 3 presents the FTIR spectra measured between 5000 and 2000 cm^{-1}. A comparison of observed and calculated energy levels and their assignments in tetragonal (S_4, D_{2d}) and cubic (T_d) symmetry together with the corresponding parental free ion terms is given in Table 4.

Three main regions of absorption around 3500, 7000, and 17,000 cm^{-1} are typical for high-spin Co^{2+} ions (d^7 configuration) in tetrahedral (T_d) or pseudotetrahedral crystal fields, where electric dipole transitions are partially Laporte-allowed due to the absence of a center of symmetry. In pure T_d symmetry these three band systems generally correspond to spin-allowed transitions from the $^4A_2(F)$ ground state to $^4T_2(F)$, $^4T_1(F)$, and $^4T_1(P)$ excited states, respectively. However, a first inspection of the polarization behavior of the π and σ spectra indicates that—in spite of the nearly perfectly regular shape of the CoO_4 tetrahedron

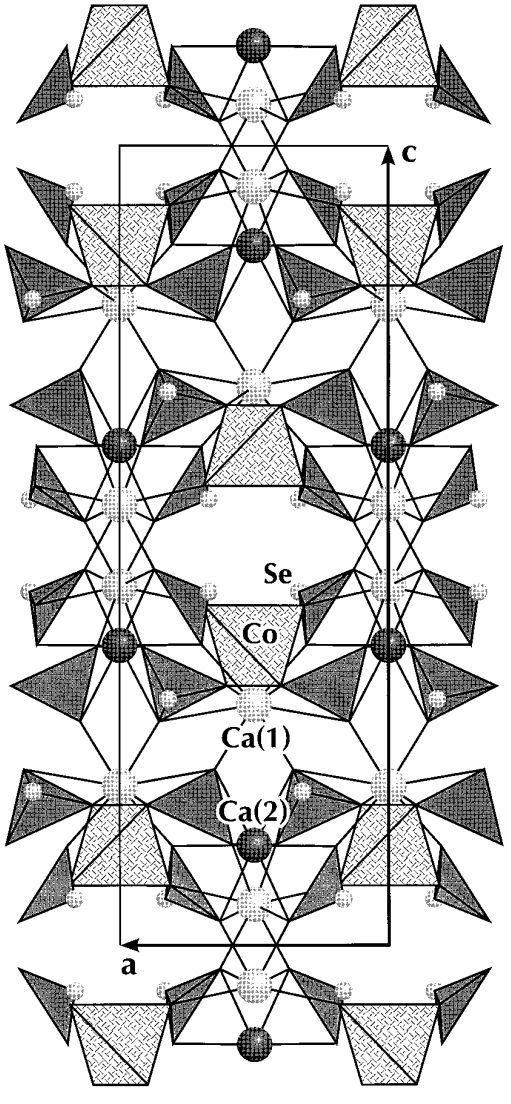

FIG. 1. Projection of the crystal structure of $Ca_3Co(SeO_3)_4$ on (010).

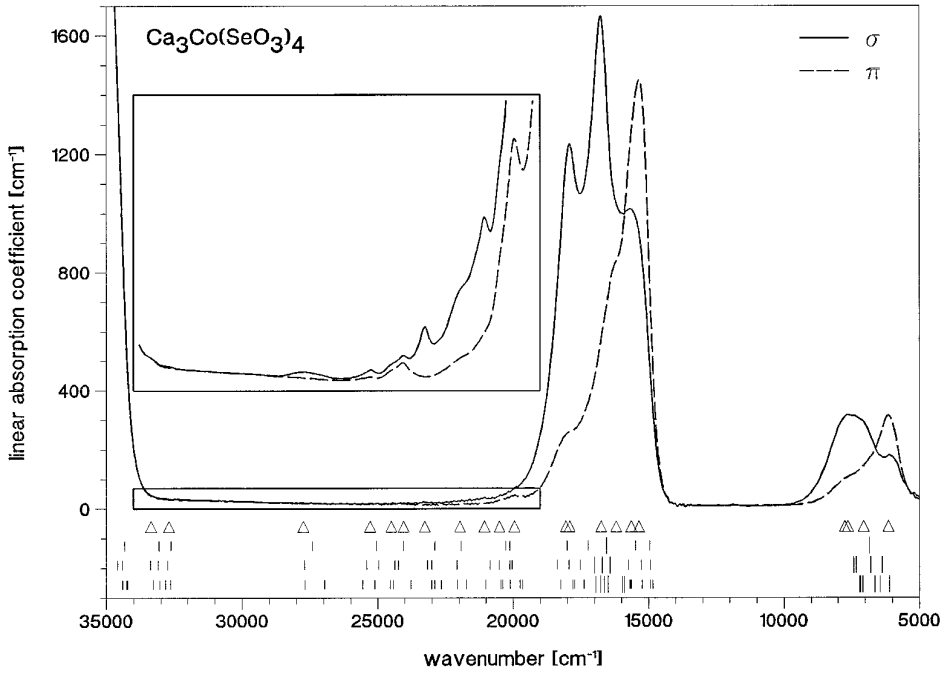

FIG. 2. Polarized absorption spectra of $Ca_3Co(SeO_3)_4$ in the region from 5000 to 35,000 cm^{-1}; sample thickness: 15 μm. Insert: ordinate-expanded spectral region from 19,000 to 34,000 cm^{-1}; sample thickness: 273 μm. Triangles indicate observed spectral features, and shorter and longer line marks represent calculated energy levels with predominant doublet and quartet character, respectively; first row: cubic approximation without spin–orbit coupling (Dq = 395, B = 770, C = 3400 cm^{-1}); second row: cubic approximation with spin–orbit coupling (Dq, B, C as before, ζ = 500 cm^{-1}); third row: tetragonal calculation as listed in Table 4 (Dq, B, C, ζ as before, Dt = 25, Ds = 250 cm^{-1})

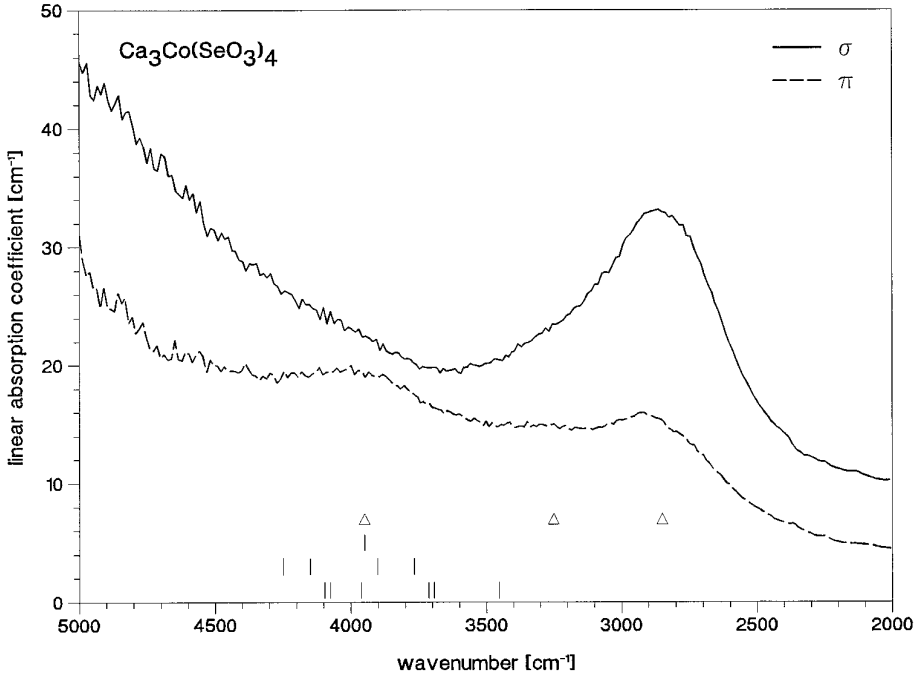

FIG. 3. Polarized FTIR absorption spectra of $Ca_3Co(SeO_3)_4$ in the region from 2000 to 5000 cm^{-1} (in this drawing the resolution is reduced from 4 to 12 cm^{-1}); sample thickness: ~240 μm. Triangles and line marks as in Fig. 2.

TABLE 4

Polarization Behavior and Energies of Spectral Features Observed in $Ca_3Co(SeO_3)_4$ and Calculated Energy Levels (Kramers Doublets) with Corresponding Tetragonal and Cubic Assignments (Parental Free Ion Terms in Parentheses)

	Energy [cm^{-1}]		Assignment			Energy [cm^{-1}]		Assignment	
Pol.	Obs.	Calc.	S_4 (D_{2d})	T_d	Pol.	Obs.	Calc.	S_4 (D_{2d})	T_d
		0	$B_{(1)}$	$^4A_2(F)$			19656	E	$^2T_2(H)$
		2					19744		
					∥	19950	−20106	$B_{(2)}$	
⊥	2850 ?	3453							
⊥, ∥	3250	3693	E		⊥, ∥	20500	20388	$A_{(2)}$	$^2T_1(H)$
		3713					20449	E	
		3962		$^4T_2(F)$	⊥	21060	−21019		
∥	3950	4074	$B_{(2)}$		⊥, ∥	21970	21729	$B_{(1)}$	$^2E(H)$
		4096					22075	$A_{(1)}$	
∥	6140	6103	$A_{(2)}$				22666	$A_{(2)}$	$^2T_1(P)$
		6454			⊥	23270	22908	E	
⊥	7050	6641		$^4T_1(F)$			23017		
⊥	7630	7080	E		∥, ⊥	24050	23772	E	$^2T_1(H)$
⊥, ∥	7750	7174					23776	$A_{(2)}$	
		7200					24429		
		14850	$A_{(1)}$	$^2E(G)$	⊥, ∥	24500			
		14951	$B_{(1)}$				24546	$B_{(2)}$	$^2T_2(D2)$
∥, ⊥	15360	15244	E	$^2T_1(G)$	⊥	25280	25110	E	
⊥, ∥	15650	15648					25570		
		15693	$A_{(2)}$				26975	$B_{(1)}$	$^2E(D2)$
∥	16200	15909	$A_{(2)}$		⊥	27750	−27686	$A_{(1)}$	
		15981			⊥	32700	32639	$B_{(1)}$	$^2A_2(F)$
		16502		$^4T_1(P)$			32835	$B_{(2)}$	$^2T_2(F)$
⊥	16760	16644	E		⊥, ∥	33500	33040	E	
		16773					33275		
		16958				~34000	onset of CT absorption edge		
		17389	$A_{(1)}$	$^2A_1(G)$			34210	$A_{(2)}$	$^2T_1(F)$
⊥	17910	17730	E	$^2T_2(G)$			34241	E	
		17796					34404		
∥	18050	−18239	$B_{(2)}$						

Note: Levels derived from the ^{2}D1 term are not included, they have energies calculated between 50084 and 52184 cm^{-1}. For a graphical representation of observed and calculated energies see Figs. 2 and 3. Parameters used for calculation: $Dq = 395$, $Dt = 25$, $Ds = 250$, $B = 770$, $C = 3400$, $\zeta = 500$ cm^{-1}.

found by the structure analysis—a rather anisotropic crystal field with a significant tetragonal component is effective on the Co^{2+} ions in $Ca_3Co(SeO_3)_4$. Obviously, in the case of the weak tetrahedral crystal field the influence of the further coordination of the CoO_4 polyhedron is more pronounced than in the stronger octahedral field. A tetragonal field component splits the T terms in an A (or $B)_{(2)}$ and an E component; the ground state A_2 transforms as $B_{(1)}$. The observed polarization behavior can then be roughly explained by the symmetry selection rules for the actual Co^{2+} point symmetry S_4 (ground state B; allowed transitions: $B \rightarrow A$: ∥, $B \rightarrow E$: ⊥), and similarly by those for D_{2d}, the symmetry of the CoO_4 polyhedron (ground state B_1; allowed transitions $B_1 \rightarrow A_2$: ∥, $B_1 \rightarrow E$: ⊥). Nevertheless, as will be shown below, a tetragonal field component alone cannot account for the observed large band splittings and band widths in the spectra of $Ca_3Co(SeO_3)_4$. Hence, an assignment based on crystal field calculations in terms of the crystal field strength Dq, the electron repulsion parameters Racah B and C, a minor perturbation by a tetragonal field component (employing the parameters Dt and Ds), and further band splitting and broadening due to spin–orbit coupling (spin–orbit coupling constant ζ) is attempted. Spin–orbit coupling totally splits all tetragonal levels into Kramers doublets which remain degenerate in the absence of a magnetic field. Furthermore, for the prominent band system in the visible region an admixture of intensity-enhanced spin-forbidden quartet → doublet tran-

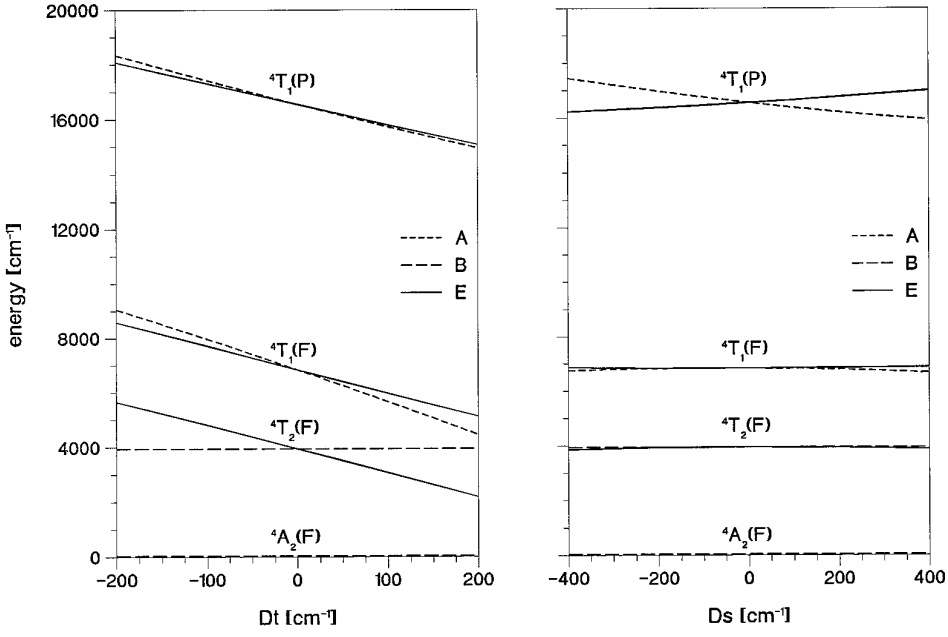

FIG. 4. Energy levels of spin-allowed transitions of Co^{2+} ions in (pseudo)tetrahedral crystal fields (Dq = 395, B = 770 cm^{-1}) as a function of the tetragonal parameters Dt (left, $Ds = 0$) and Ds (right, $Dt = 0$). For $Dt = Ds = 0$ cubic assignments with parental free ion terms in parentheses are given.

sitions into the spin allowed $^4T_1(P)$ transition is assumed (Table 4).

The band system in the IR region with components centered at about 3950, 3250, and 2850 cm^{-1} (Fig. 3) can be assigned, at least in part, to the transition $^4A_2 \rightarrow {}^4T_2$ (in T_d), where both levels arise from the free ion ^4F term. In fact, this transition is electric-dipole forbidden in T_d symmetry, explaining the low intensity of absorption. The origin of the band component at 2850 cm^{-1} (and of the weak feature at 3250 cm^{-1}) is uncertain. The polarization behavior suggests that it represents the tetragonal E split component of $^4T_2$. The very weak band centered at 3950 cm^{-1} is then assigned to the $B_{(2)}$ level of $^4T_2$ and thus definitely fixes the value of Dq at 395 cm^{-1}. However, the large splitting of ~1100 cm^{-1} can hardly be explained, neither by splitting due to spin–orbit coupling, nor by a tetragonal field component: in a first approximation, the tetragonal splitting of $^4T_2$ depends only on the magnitude of Dt (Fig. 4), in the present case leading to $Dt \approx 120$ cm^{-1}, a value which prevents a good agreement of observed and calculated energies of higher crystal field levels (Fig. 4 shows that both $^4T_1$ levels are strongly shifted to lower energies with increasing Dt). Due to strong vibrational absorption of many polyatomic ligands in the mid-IR region, components of the $^4A_2 \rightarrow {}^4T_2$ transition have only been occasionally observed so far, and these measurements were rarely extended to energies below ~3700 cm^{-1}. Such examples are the spectra of Co doped in ZnS and CdS (16), of Co incorporated at the eightfold site in CaF_2 (with a field strength comparable to tetrahedral complexes) (17), and Co in sodium silicate glasses, $Na_2O \cdot xSiO_2$ (x = 1.5–3.0) (18). While the sulfide spectra exhibit no details within the region covered in Fig. 3, the latter two show each two absorption bands with intensities and band widths comparable to $Ca_3Co(SeO_3)_4$. The low energy components are centered at 2950 cm^{-1} in CaF_2 and at 2800 cm^{-1} in $Na_2O \cdot 2SiO_2$ and attributed to effects not caused by Co^{2+} ions (17) and to a spin–orbit split-level of $^4T_2$ (18). As mentioned already above, this explanation cannot account for the large splitting in $Ca_3Co(SeO_3)_4$. On the other hand, an assignment of the band at 2850 cm^{-1} to the stretching frequency of OH dipoles, which might perhaps be incorporated in trace amounts in the structure of $Ca_3Co(SeO_3)_4$, is not consistent with the OH content estimated from the integrated intensity of this band as well as with interatomic O–O distances available for hypothetical hydrogen bonds (cf. 19). Therefore, the origin of the feature at 2850 cm^{-1} must remain suspect.

The band system which covers the spectral region from about 6000 to 8000 cm^{-1} is attributed to the $^4A_2 \rightarrow {}^4T_1(F)$ transition in T_d symmetry. Discernible components are located at 6140, 7050, and around 7700 cm^{-1}. The low energy level is π polarized, while the high energy components are mainly σ polarized, indicating that the tetragonal field considerably splits the $^4T_1(F)$ state into a lower $A_{(2)}$ and a higher E level. This splitting scheme is inverse to

that discussed above for the $B_{(2)}$ and the presumed E split level of the $^4T_2$ state; both tendencies can be accounted for in crystal field calculations using a positive value for the parameter Dt. The magnitude of Dt is limited by the strong red-shift of both $^4T_1$ split components with increasing Dt (Fig. 4) and is very roughly estimated to be $\approx$25 cm^{-1}. The inclusion of spin–orbit coupling in the crystal field calculations with $\zeta = 500$ cm^{-1} and setting $Ds \approx 250$ cm^{-1} (see below) an overall splitting of the $^4T_1(F)$ state of $\sim$1100 cm^{-1} is calculated (Table 4). Nevertheless, this is significantly less than the observed splitting of $\sim$1600 cm^{-1}. A comparable situation is found for observed and calculated energies of the $^4T_2(F)$ manifold.

Typically, the prominent absorption bands located in the visible part, in $Ca_3Co(SeO_3)_4$ spanning the region from about 15,000 to 18,500 cm^{-1}, are by far the most intense in the electronic spectra of Co^{2+} in tetrahedral coordination. Distinct maxima or shoulders are observed at 15,360, 15,650, 16,200, 16,760, 17,910, and 18,050 cm^{-1}. The assignment of the components of this manifold is seriously complicated by the overlap of the spin-allowed $^4A_2 \rightarrow {}^4T_1(P)$ (T_d) transition with spin-forbidden transitions to split levels derived from the ^2G free ion term. Due to the effect of spin–orbit coupling, the latter can "steal" a considerable portion of intensity from the spin-allowed transition. An approximate location of the $^4T_1(P)$ state may be deduced from the polarization behavior of the band system, which should be governed by the spin-allowed transition and which corresponds to the situation of the NIR absorption band; i.e., $^4T_1(P)$ is split by the tetragonal field component into a lower $^4A_{(2)}$ and a higher ^4E level. The ^4E level is assumed to be correlated with the central peak in the σ spectrum at 16,760 cm^{-1}; the $^4A_{(2)}$ level may be located near the center of the band envelope in the π spectrum at about 16,000 cm^{-1}. Since this splitting in first order depends on the tetragonal parameter Ds (Fig. 4), it is roughly estimated that $Ds \approx 250$ cm^{-1}. The position of the $^4A_2 \rightarrow {}^4T_1(P)$ transition also fixes the value of the electron repulsion parameter Racah B at $B = 770$ cm^{-1}. The energies of the spin-forbidden transitions depend on both Racah parameters, B and C, and with $C = 3400$ cm^{-1} a rather good agreement between observed and calculated energies can be obtained (Fig. 2 and Table 4). The peak maximum at 15,360 cm^{-1} in π and the intense shoulder at 15,650 cm^{-1} in σ are then assigned to components of the spin forbidden $^2T_1(G)$ state, which gain up to about 25% quartet character from the $^4T_1(P)$ level. The $^2E(G)$ state is calculated to lie within the low energy ascent of the visible band. It is not explicitly observed, but probably contributes to the absorption. The band features on the high energy side around 18,000 cm^{-1} can be correlated with intensity enhanced transitions to the $^2T_2(G)$ state; the $^2A_1(G)$ level may also contribute. In the region between 20,000 cm^{-1} and the outset of the charge transfer absorption edge at about 34,000 cm^{-1} several weak spectral features are observed (insert in Fig. 2) which can be correlated reasonably well with spin-forbidden quartet $\rightarrow$ doublet transitions to energy levels derived form the higher free ion terms ^2H, ^2P, $^2D2$, and ^2F (Table 4). In the crystal field the ^2H, ^2P, and $^2D2$ terms are considerably mixed; in Table 4 the character of the parental free ion term is given. With the increase of the energy gaps between the doublet levels and the spin-allowed $^4T_1(P)$ state, the admixture of quartet character to the doublets decreases. This is in accordance with the continuous decrease in absorption intensity of higher spin-forbidden transitions. Obviously, the intensity enhancement due to energetically higher charge transfer processes is negligible.

The crystal field and electron repulsion parameters derived above by direct observation (Dq), by a kind of "fitting" process (Racah B and C), or by estimation (ζ, Dt, Ds) are generally in good agreement with values expected for Co^{2+} ions in (pseudo-)tetrahedral coordination by oxygen ligands. Values of the crystal field strength parameter Dq for $Co^{2+[4]}$ in oxygen based crystal structures or glasses are quite similar to $Dq = 395$ cm^{-1} found in $Ca_3Co(SeO_3)_4$; e.g., for Co^{2+} diluted in the structure of ZnO Dq values of 390 cm^{-1} (16, 20) or 400 cm^{-1} (21) are reported. The spectra of Co^{2+} in $MgAl_2O_4$ and $ZnAl_2O_4$ spinels (16, 22) yield $Dq = 400$ and 410 cm^{-1}, respectively. Somewhat higher values were reported for Co^{2+} in garnets ($Dq = 460$ cm^{-1}) (23) and, obtained from solution spectra, for the $[Co(OH)_4]^{2-}$ complex ($Dq = 423$ cm^{-1}) (24) and the $[Co(NO_3)_4]^{2-}$ complex ($Dq = 466$ cm^{-1}) (25). For the latter, however, it was shown that the central Co is actually eight-coordinated (26), thus explaining the deviation of Dq. For Co^{2+} in glasses values comparable to those of the single crystals are observed: in Li_3PO_4 glass, for example, Dq is 400 cm^{-1} (27). Nelson and White (18) investigated various glasses with composition $Na_2O \cdot 1.5$–$3SiO_2$ where Dq is very constant at 378–379 cm^{-1}, while in a number of borate, phosphate, germanate, and other glasses Dq ranges 381–452 cm^{-1}. In albite and albite–diopside glasses (28) Dq is 383 and 404 cm^{-1}, respectively.

The influence of the crystal field on the values of the Racah parameters B and C gives an approximate indication of the covalent contribution to bonding. As found for Dq, the parameters $B = 770$ cm^{-1} and $C = 3400$ cm^{-1} as well as the resulting values for the nephelauxetic ratio $\beta = 0.79$ [$\beta = B/B_0$, where $B_0 = 971$ cm^{-1}, the Co^{2+} free ion value (29)] and the ratio $C/B = 4.42$ are consistent with relevant data from literature: in the single crystals mentioned above B ranges from 700 to 775 cm^{-1} (for ZnO the somewhat contradictory values 700, 760, and 775 cm^{-1} are given in Refs. (20, 21, 16), respectively), in most of the glasses from about 750 to 790 cm^{-1} (18, 28). C/B is generally assumed or derived to scatter closely around 4.5.

As is the case—without exception—for the Racah pa-

rameters, also the spin–orbit coupling constant should be reduced in the crystal field from the Co^{2+} free ion value $\zeta_0 = 540\ cm^{-1}$. In $Ca_3Co(SeO_3)_4$, ζ is set to 500 cm^{-1} which represents 92% of the free ion value. In the literature mostly values between 400 and 500 cm^{-1} are cited. Nevertheless, in order to account for the very large splittings and widths of both $^4T_1$ band systems, some authors postulate a value for ζ which is larger than the free ion value. As an example, Weakliem (16) gives $\lambda = -210$, i.e., $\zeta = 630\ cm^{-1}$, for Co in ZnO and $MgAl_2O_4$. However, in the present case, the splitting in the visible band manifold is interpreted in terms of a superposition of intensity enhanced doublet states and the $^4T_1(P)$ state, and in crystal field calculations with $\zeta = 650\ cm^{-1}$, an improved agreement of observed and calculated energies within the $^4T_1(F)$ level is counterbalanced by a worsened agreement in the VIS and UV region.

The values of the tetragonal crystal field parameters, *Dt* and *Ds*, both may be considerably in error, but at least their positive signs seem to be established quite definitely by the polarization behavior of the spectra of $Ca_3Co(SeO_3)_4$.

ACKNOWLEDGMENTS

The author is greatly indebted to the Alexander von Humboldt-Stiftung, Bonn-Bad Godesberg, for a research fellowship at the Technische Universität Berlin, where the optical spectra were measured. Many thanks are due to Professor K. Langer, Berlin, for valuable discussions and to Dr. M. Andrut, Berlin, for helpful discussions and technical assistance. H. Reuff, Berlin, carefully prepared the crystals for the microscope-spectrometric measurements. The author further thanks Professor A. Beran, Vienna, for his help with the FTIR measurements and for discussions concerning these results, as well as Professor E. Tillmanns, Vienna, for helpful comments. Partial financial support for the FTIR and structural investigations at the Vienna University was provided by JCPDS Grant ET90-03.

REFERENCES

1. M. Wildner, *J. Solid State Chem.* **115,** 360 (1995).
2. M. Wildner, *J. Solid State Chem.* **120,** 182 (1995).
3. M. Wildner, *Z. Kristallogr. Suppl. Issue* **9,** 248 (1995).
4. L. Banci, A. Bencini, C. Benelli, D. Gatteschi, and C. Zanchini, *Structure Bonding* **52,** 37 (1982).
5. A. B. P. Lever, "Inorganic Electronic Spectroscopy," 2nd. ed. Elsevier, Amsterdam, 1984.
6. M. Wildner and K. Langer, *Phys. Chem. Miner.* **20,** 460 (1994).
7. M. Wildner and K. Langer, *Phys. Chem. Miner.* **21,** 294 (1994).
8. Stoe & Cie, "STRUCSY—Structure System Program Package", Stoe & Cie, Darmstadt, 1984.
9. G. M. Sheldrick, "SHELXL-93, A Program for Crystal Structure Refinement." Univ. Göttingen, 1993.
10. K. Langer and K. R. Fentrup, *J. Microscopy* **116,** 311 (1979).
11. Y. Y. Yeung and C. Rudowicz, *Computers Chem.* **16,** 207 (1992).
12. F. C. Hawthorne, L. A. Groat, and T. S. Ercit, *Acta Crystallogr. C* **43,** 2042 (1987).
13. M. Wildner, *Z. Kristallogr.* **202,** 51 (1992).
14. W. H. Baur, *in* "Structure and Bonding in Crystals" (M. O'Keeffe and A. Navrotsky, Eds.), Vol. II, p. 31–52. Academic Press, New York, 1981.
15. N. E. Brese and M. O'Keeffe, *Acta Crystallogr. B* **47,** 192 (1991).
16. H. A. Weakliem, *J. Chem. Phys.* **36,** 2117 (1962).
17. R. Stahl-Brada and W. Low, *Phys. Rev.* **113,** 775 (1959).
18. C. Nelson and W. B. White, *J. Mater. Res.* **1,** 130 (1986).
19. K. Nakamoto, M. Margoshes, and R. E. Rundle, *J. Am. Chem. Soc.* **77,** 6480 (1955).
20. R. Pappalardo, D. L. Wood, and R. C. Linares, *J. Chem. Phys.* **35,** 2041 (1961).
21. P. Koidl, *Phys. Rev. B* **15,** 2493 (1977).
22. J. Ferguson, D. L. Wood, and L. G. van Uitert, *J. Chem. Phys.* **51,** 2904 (1969).
23. D. L. Wood and J. P. Remeika, *J. Chem. Phys.* **46,** 3595 (1967).
24. F. A. Cotton, D. M. L. Goodgame, and M. Goodgame, *J. Am. Chem. Soc.* **83,** 4690 (1961).
25. F. A. Cotton and T. G. Dunne, *J. Am. Chem. Soc.* **84,** 2013 (1962).
26. F. A. Cotton and J. G. Bergman, *J. Am. Chem. Soc.* **86,** 2941 (1964).
27. M. Berretz and S. L. Holt, *J. Inorg. Nucl. Chem.* **36,** 49 (1974).
28. H. Keppler, *Am. Miner.* **77,** 62 (1992).
29. Y. Tanabe and S. Sugano, *J. Phys. Soc. Jpn.* **9,** 766 (1954).